New measurements of the two-photon absorption in GaP, CdS, and ZnSe relative to Raman cross sections

Cid B. de Araujo* and Haim Lotem†

Gordon McKay Laboratory, Harvard University, Cambridge, Massachusetts 02138
(Received 29 December 1977)

The two-photon absorption (TPA) coefficient in GaP, CdS, and ZnSe was measured at 3.56 eV using the TPA normalization technique and at 3.18 eV using a new calibration method. In this method the TPA effect is normalized by comparing the two-photon nonlinear attenuation with stimulated Raman gain in materials with known Raman cross section. By utilizing different Raman modes, reliable TPA cross sections, independent of the laser characteristics, are obtainable. When combined with recently published cross sections at 3.91 eV the TPA results at 3.18 and 3.56 eV show interesting spectroscopic features.

I. INTRODUCTION

The two-photon absorption (TPA) processes in condensed matter have been the subject of extensive experimental and theoretical investigations in the recent years.[1,2] The main reason for such interest is that the investigation of two-photon transitions extends the capabilities of the one-photon (linear) spectroscopy. A large variety of nonlinear (NL) phenomena like TPA, stimulated Raman scattering, and self-focusing and parametric mixing processes may be described in terms of a third-order NL susceptibility $\chi^{(3)}$.[3-5] This material parameter is perhaps as basic as the complex linear dielectric constant. A major spectroscopic difference between the third-order susceptibility and the complex dielectric constant is that the former material parameter is sensitive to one-photon as well as to two-photon transitions such as Raman and TPA processes. Because of these important spectroscopic characteristics and the fact that $\chi^{(3)}$ is a fourth-rank tensor, a complete determination of $\chi^{(3)}$ may give, in principle, more information on the material system than the linear spectroscopic methods give. Isotropic systems are, for example, characterized by one dielectric constant and by three independent coefficients of $\chi^{(3)}$.[2,6]

The lowest-order NL susceptibility $\chi^{(2)}$ must also be regarded as a basic material spectroscopic parameter. However, in contrast with $\chi^{(3)}$, which is in general nonzero, $\chi^{(2)}$ vanishes in media with a center of inversion. $\chi^{(2)}$ is sensitive to one- and two-photon resonances of the material, with the two-photon resonances in $\chi^{(2)}$ being accompanied by coincidental one-photon resonances. This characteristic introduces severe difficulties in the experimental determination of the second-order susceptibility in regions above the fundamental energy gap of the material.[7] $\chi^{(3)}$ may therefore be

regarded as a more general spectroscopic parameter of matter.

The classical methods for measuring $\chi^{(3)}$ utilize stimulated processes in which the material system changes its quantum state. The imaginary part of $\chi^{(3)}$ may be directly measured by the NL attenuation or gain caused by the TPA or Raman transitions, respectively. Both these effects are proportional to the imaginary part of $\chi^{(3)}$. The real part of $\chi^{(3)}$ which is responsible, for example, for the effect of self-focusing, may be directly and accurately obtained by interferrometric methods recently reported by Owyoung.[8]

Parametric mixing processes[3] may also be described in terms of $\chi^{(3)}$. These processes, by which energy is transferred between different components of the interacting electromagnetic fields, are not accompanied by a change in the material quantum state. New parametric mixing experimental techniques allow us to measure the real and imaginary part of $\chi^{(3)}$. For example, by the coherent anti-Stokes Raman scattering methods, the real part of the TPA resonance contribution to $\chi^{(3)}$ in organic liquids has been obtained in quite a routine way.[9,10] However, it is less convenient to obtain by this method the imaginary part of this susceptibility which corresponds to the TPA contributions.[10]

Methods based on direct NL attenuation are generally inaccurate because of the critical dependence of the measurements on the exact parameters of the lasers utilized in the experiments. This experimental difficulty is reflected in the large scattering of the TPA results reported in the literature, as discussed in Refs. 11–13. Recently developed normalization techniques solve this experimental difficulty.[11,12]

In this paper we present a new method (the composite sample technique) for direct and reliable calibration of TPA coefficients via Raman-gain

measurement. This technique is based on destructive interference between the Raman contribution (gain) and the TPA contribution (loss) in a composite sample consisting of the investigated two-photon absorber in series with a known Raman-active material. For a probe beam at ω_p and a strong beam at ω_L the destructive interference occurs because the sign of the TPA coefficient, which is proportional to $\mathrm{Im}\,\chi^{(3)\prime}(-\omega_p, \omega_p, \omega_L, -\omega_L)$, is opposite to the sign of the Raman gain, which is also proportional to the imaginary part of the same susceptibility in the Raman-active material. Destructive or constructive interference between Raman and TPA contributions to $\mathrm{Im}\,\chi^{(3)}$ may be obtained with $\omega_L - \omega_p > 0$ and $\omega_L - \omega_p < 0$, respectively. A clear observation of this interference effect in $\chi^{(3)}$ was recently reported.[14] Competition between Raman and TPA contributions in a stimulated Raman scattering (SRS) experiment has been seen by El-Sayed et al.[15] They explain the observed changes in the SRS threshold versus laser frequency by a cascade process in which the Stokes photons are absorbed via the TPA process. The formalism of NL susceptibilities naturally explains their observations. The third-order susceptibility of Raman-active materials includes both Raman and two-photon resonance contributions. Whenever the latter ones are of the same magnitude or larger than the Raman contributions the SRS effect is quenched.

The effect of destructive interference is used in the composite sample calibration technique for TPA cross-section calibration versus known Raman cross sections. This technique is complementary to the TPA calibration versus the inverse Raman effect described in Ref. 11. The latter method is performed with $\omega_L - \omega_p < 0$ and hence the Raman term contributes to NL absorption. Using both of these calibration techniques, one strong laser at ω_L may be used for obtaining TPA spectra in the range $[(2\omega_L - \omega_R), (2\omega_L + \omega_R)]$, where ω_R is a Raman frequency in a liquid of the order of 3000 cm^{-1}. Because a Raman reference material is used in the composite sample technique, this method does not depend on the properties of the lasers and the TPA cross sections may be obtained with no need for calibration of the laser intensity.

In this paper, the TPA cross sections of CdS, ZnSe, and GaP at 3.18 eV were calibrated relative to the Raman cross section of the 3063 cm^{-1} mode of benzene. In addition, the TPA coefficients of those materials were obtained at 3.56 eV by the normalization technique.[12]

The present results and the results of Ref. 11 are compared to simplified theoretical calculations based on the Keldysh theory of multi-photon transitions[16] and Basov's model for TPA.[17]

II. THEORY

The TPA attenuation (or Raman gain) at ω_p induced by a strong laser at ω_L is described by

$$\frac{dI_P(x,y,z,t)}{dz} = -[\alpha + \beta I_L(x,y,z,t)]I_P(x,y,z,t), \qquad (1)$$

where α is the one-photon absorption coefficient of the sample at ω_p and

$$\beta = (32\pi^2 \omega_p/c^2 \eta_p \eta_L)\,\mathrm{Im}\,\chi_{xxxx}^{(3)}(-\omega_p, \omega_p, \omega_L, -\omega_L). \qquad (2)$$

The macroscopic susceptibility $\chi^{(3)}$ may be described in terms of a microscopic hyperpolarizability, $\gamma^{(3)}$,

$$\chi_{ijkl}^{(3)} = NL\gamma_{ijkl}^{(3)}, \qquad (3)$$

where N is the number of unit cells in unit volume and L is the local field correction. The contribution of the TPA process to γ may be calculated using the density matrix perturbation expansion. The element $\gamma_{ijkl}^{(3)}$ is given by

$$\gamma_{ijkl}^{(3)}(-\omega_p, \omega_p, \omega_L, -\omega_L)$$

$$= \sum_{g,t} \rho_{gg}^0 \frac{g_{il}(\omega_p, \omega_L)f_{jk}(\omega_p, \omega_L)}{\omega_{tg} - (\omega_p + \omega_L) - i\Gamma_{tg}}, \qquad (4)$$

where

$$g_{xy}(\omega_p, \omega_L) = \left(\frac{6}{\hbar^3}\right)^{1/2} \sum_h \left(\frac{P_{gh}^x P_{ht}^y}{\omega_{hg} - \omega_p - i\Gamma_{hg}}\right.$$

$$\left. + \frac{P_{gh}^y P_{ht}^x}{\omega_{hg} - \omega_L + i\Gamma_{hg}}\right),$$

$$\qquad (5)$$

$$f_{xy}(\omega_p, \omega_L) = \left(\frac{6}{\hbar^3}\right)^{1/2} \sum_h \left(\frac{P_{th}^x P_{hg}^y}{\omega_{hg} - \omega_L - i\Gamma_{hg}}\right.$$

$$\left. + \frac{P_{th}^y P_{hg}^x}{\omega_{hg} - \omega_p - i\Gamma_{hg}}\right).$$

In these equations h, g, and t represent the material energy levels, $\vec{P}$ is the dipole moment operator, $\hbar\omega_{hg}$ is the energy difference between levels h and g, the factor $\Gamma_{hg} > 0$ is the damping of the off diagonal term ρ_{hg}, and ρ_{gg}^0 is the population of level g. It is assumed that the variation in the population of the various energy levels, i.e., saturation effects, may be ignored.

An additional effective term in $\chi^{(3)}$ may originate from a second-order mixing process in solids in which $\chi^{(2)}$ is nonzero. This term is an indistinguishable part of the effective measured $\chi^{(3)}$. Thus, the effective third-order NL susceptibility may be written as a sum of a direct third-order

and a two-step second-order mixing contributions. For the case of a single beam TPA experiment[6,18,19] we have

$$\chi_{ijkl}^{(3)\text{eff}} = \chi_{ijkl}^{(3)} + \tfrac{2}{3}\chi_{ijm}^{(2)}\chi_{mkl}^{(2)}\frac{4\pi}{\epsilon(2\omega_L) - \epsilon(\omega_L)}, \qquad (6)$$

where $\epsilon(\omega_j)$ are the dielectric coefficients. The latter expression may be easily generalized to the case of a two beam experiment. The second-order mixing term [second term in Eq. (6)] depends on the beam direction as well as on the beam polarization.

From Eqs. (4) and (5) it is clear that $\chi^{(3)}$ is sensitive to both one- and two-photon transitions of the material. The TPA spectrum may therefore give information on both these transitions. In principle, it is much simpler to analyze linear spectra than to analyze spectra of $\chi^{(2)}$ or $\chi^{(3)}$, because the linear spectra may be combined into contributions from pairs of bands.[6] The contributions to $\chi^{(2)}$ or to $\chi^{(3)}$ [as seen in Eqs. (4) and (5)] are more complicated. In the NL case the intermediate states play an important role in the susceptibility, in addition to the initial and final states. In solids, for example, regions in the Brillouin zone which have relatively high weight in the contribution to $\chi^{(1)}$ may become less important to $\chi^{(3)}$ and vice versa. In a system with a center of inversion the spectra of one-photon absorption as a function of $\hbar\omega$ and the TPA as a function of $\hbar(\omega_1 + \omega_2)$ are different because final states of different parity are involved. If the crystal has no inversion symmetry, some peaks will be common to both spectra. Thus, we can obtain more information about energy-band structure by combining one-photon absorption and TPA measurements.

An interesting spectral region in the TPA measurements is the double resonance region in which one- and two-photon transitions are simultaneously close to resonance. In this case, interference effects between different TPA contributions to $\chi^{(3)}$ may be observed. An analogous double-resonance process in $\chi^{(3)}$ is the resonance Raman effect in which the cross section of selected Raman modes is enhanced as the laser frequency is tuned close to the one-photon energy gap of the material. Experimentally, both these double-resonance effects are hard to analyze because of saturation caused by the linear absorption.

Actual calculations of $\chi^{(3)}$ are very difficult to perform because the detailed description of the wave functions and the eigenvalues needed for these calculations is not available for most physical systems. Rigorous calculations of $\chi^{(3)}$ may be performed, however, in atomic systems when one- and two-photon transitions are simultaneously close to resonance. In this near-double-resonance case the calculation is relatively simple since in many atomic systems only a few matrix elements and energy levels are relevant to the calculation. The situation is much more complicated in molecular systems and condensed matter because of the complexity of these quantum systems.

In order to calculate optical parameters in solids over a wide spectral range the detailed band structure with transition-matrix elements over the entire Brillouin zone is needed. A successful technique for calculating these material parameters is the empirical pseudopotential method[20,21] (EPM). Good theoretical results have been obtained in describing linear spectral data of solids using this technique. In spite of the large number of published experimental works on TPA cross sections in solids only limited attempts have been made to use detailed material band structure in the calculation of $\chi^{(3)}$. The large scattering of the reported experimental results (close to three orders of magnitude) for those crystals that had been extensively explored[1,14] did not provide incentive to improve the theory. Most of the reported calculations used a simplified band-structure model for the material, where the $\vec{k}$ dependence of the momentum matrix elements is neglected. These approximations may give good estimates for $\chi^{(3)}$ and for the dispersion of $\chi^{(3)}$ only in the spectral region where the two-photon energy is close to the band edge of the material at the center of the Brillouin zone. Above the fundamental band gap important contributions to $\chi^{(3)}$ originate from different singular points in the Brillouin zone. Since the simple models do not take into account the band shape in the vicinity of these singular points, their predictions for $\chi^{(3)}$ in spectral regions above the gap energy are not reliable.

In the theoretical estimates of β performed in this work, we have used the models of Basov[17,22] and Keldysh.[16,22] As is the case in the models mentioned above, the material system is described by a simplified band structure. In Basov's model one essentially integrates Eq. (4) for a simple parabolic band structure, with constant matrix elements. Keldysh uses an approach different from the standard perturbation treatment. In his model, one first calculates the effect of the electromagnetic perturbation on the eigenstates of the system. Then the transition rate is calculated between the perturbed states. The latter model is especially useful for high-order multiphoton transition rates.[23] Because the models used here give β as a function of 2ω while the measurements were done at $\omega_L + \omega_p = 2\omega$, the calculated results are corrected for the trivial ω_p factor in β [see Eq. (2)]. This correction is reasonable because we are far from one-photon resonance conditions and therefore the one-
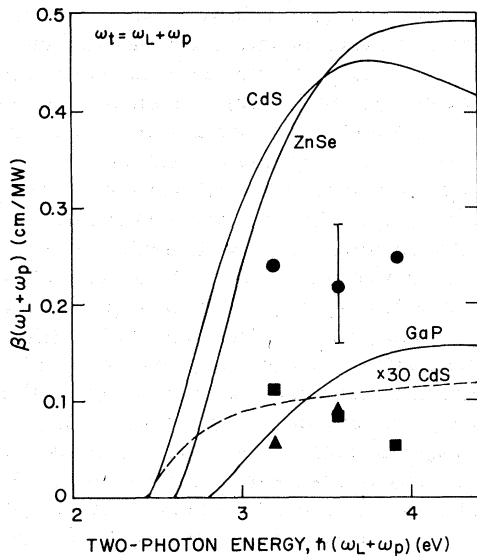
FIG. 1. TPA coefficient of CdS (■), GaP (●), and ZnSe (▲) vs the two-photon energy. The data at 3.18 eV was obtained by the composite sample method. At 3.91 eV we present the corrected data of Ref. 11 (Ref. 28) and at 3.56 eV the TPA cross sections obtained by the normalization technique were calibrated using relative TPA cross sections in TiO_2 from Ref. 29 (see text). The error bar represents a typical uncertainty of ±25% in the measured coefficients. The three solid lines describe the Basov model calculations for the three samples. The calculation based on the Keldysh model is shown for CdS with the dashed line. Similar dispersion was found in GaP and ZnSe.

TABLE I. Parameters used in the calculations of β.

Sample [a]	Energy gap (eV)	$m*/m_e$	Index of refraction
GaP	2.78	0.187 [b]	3.25
CdS	2.42	0.192 [c]	2.41
ZnSe	2.58	0.132 [c]	2.43

[a] The GaP and CdS crystals used here are the same samples used in Ref. 11, with identical orientations. The ZnSe is a polycrystalline sample.
[b] See Ref. 24.
[c] See Ref. 22.

photon dispersion in $\chi^{(3)}$ may be neglected in all the samples. In the calculations, we follow Mitra et al.[22] who made a critical study of Keldysh's and Basov's models. The calculated results in the region 2–4 eV are shown in Fig. 1. The material parameters used in the calculations are listed in Table I. The effective mass $m*$ was obtained from the measurement of transport properties. In spite of its simple assumptions, the Basov's model gives the correct order of magnitude for β in the three materials studied here. The results of Keldysh's model show the usual trend of too-small TPA cross sections.[22] Using Keldysh's model the one-photon absorption coefficient α may be also readily obtained. Using this model Mitra et al.[22] have shown that satisfactory results for the magnitude and the dispersion of α_1 could be obtained in GaAs and InSb. The magnitude of the transition matrix element in Basov's and Keldysh's is directly related to $m*$. Therefore, by varying $m*$ one can obtain the right magnitude for β.[23] We checked the values of $m*$ used in our calculations by calculating α_1 using the Keldysh's model in the spectral region close to the band gap. Good fit with the experi-

mental data was achieved in the three materials studied here, and therefore we did not vary the values of $m*$ used in the calculations in the NL case.

Detailed calculations of $\chi^{(2)}$ and $\chi^{(3)}$ based on the EPM technique were reported recently. Fong and Shen[25] have calculated $\chi^{(2)}$ in high-symmetry semiconductors. Their results are not as successful as the calculations of linear phenomena based on this model. This might show that the EPM model does not represent correctly the material characteristics, but, on the other hand, the measurements of $\chi^{(2)}$ might not reflect the material bulk properties, because of the small penetration depth of light at frequencies above the energy band gap, and the critical dependence of the determined value of $\chi^{(2)}$ on the material dielectric constants which are not very well known for frequencies above the fundamental gap. A calculation of $\chi^{(3)}$ based on a somewhat simplified EPM method has been recently reported by Koren.[26] His calculations for ZnS and ZnO show a good fit with two-photon photoconductivity dispersion measurements. However, it is not clear if these calculations give the correct magnitude of β because of the uncertainty in the absolute value of the TPA coefficient obtained by photoconductivity methods.

III. EXPERIMENTAL PROCEDURE

The experimental arrangement used in the composite sample technique is shown in Fig. 2. A probe laser beam at ω_p ($\lambda \sim 8800$ Å) monitors the effective gain at ω_p, as a function of the intensity of the strong laser at ω_L, in the composite sample. This sample consists of a two-photon absorber of thickness d_T in series with a Raman-active material in a cell of thickness d_R.

The probe beam is generated in a nearly longitudinal pumped-dye laser (see Fig. 2). Strong lasing in the vicinity of the Stokes-shifted frequency of benzene, 3063 cm^{-1} ($\lambda \sim 8817$ Å) is obtained using a 20-mm-long dye cell filled with $\sim 10^{-4}$ M solution
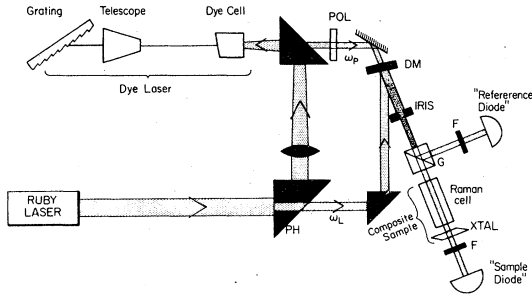
FIG. 2. Schematic diagram of the composite sample calibration experiment. The hole in prism PH is used to transmit the central part of the ruby laser beam. The dye laser output beam travels above the pump prism. POL is a glan prism which polarizes the dye laser beam at 45° to the vertical. G is a glan prism, DM is a dichroic mirror with R=100% at the ruby laser frequency, and F are cutoff filters.

of Kodak dye IR 140 dissolved in dimethyl sulfoxide (DMSO). In a 1-m-long cavity with 30:1 telescope and 1200 grooves/mm grating the lasing linewidth did not exceed 1 cm^{-1}. Since the linewidth is much smaller than the 9.4 cm^{-1} full width at half-maximum of the Raman mode used, the spontaneous Raman spectrum which was obtained with a 0.4 cm^{-1} slitwidth was used with no modification for analyzing the data. The 2855 cm^{-1} mode of cyclohexane was not used for calibration[11] because we had found it very hard to get stable lasing at $\lambda \sim 8860$ Å which corresponds to this mode of cyclohexane.

The probe beam is linearly polarized at 45° to the vertical by the glan prism (POL). The second glan prism (G) splits the probe beam into the composite sample and the reference channels. The signals are amplified, digitized, and punched on a tape which is later analyzed by a computer. The dichroic mirror (DM) is used for combining the strong ruby beam with the probe beam. The ruby beam used for inducing the nonlinearity in the sample is a small fraction of the original ruby pulse transmitted through a hole in the prism (PH). The Raman cell is a standard 10-cm-long spectroscopic cell. The filters (F) (Corning glass 5-56 and 7-69) are cutoff filters used to attenuate the ruby beam at the detectors. The detectors are 2-in. diameter biplanar ITT F4000 photodiodes. We have found that the use of large-area photodiodes is crucial in the experiment. With small photocathodes of 5 mm diameter, a scattering of the order of 10% in the linear transmitted intensity through the sample is observed. This is in spite of the reference-normalizing channel. With the larger area detectors the scattering was reduced to less than 2%. A possible explanation for this scatter-

ing is that it originates from effects connected with the multimode laser speckle which varies from shot to shot.[27]

The experimental procedure is as follows: The average value of the transmitted signal in the composite sample channel of about 15–20 laser shots is measured once in the presence of the ruby beam at the sample and once when the ruby beam is blocked. Since the ruby intensity is quite constant during a run, the magnitude of the gain (or loss) in the composite sample may be obtained at different setting of $\omega_L - \omega_p$ from the latter measurements. The probe beam intensity, which fluctuates by about 10% from shot to shot, is normalized using the reference channel.

The solution of Eq. (1) for the intensity at ω_p transmitted through the composite sample is

$$I_p(z = D) = KI_p(z = 0) \exp\left[-\beta_{\text{eff}} I_L(z = 0)\right],$$

$$\beta_{\text{eff}} = \beta^T (1 - R_R)^2 (1 - R_T)\left[1 - \exp(-\alpha_L^T d_T)\right] / \alpha_L^T$$
$$- \beta^R (1 - R_R)\left[1 - \exp(-\alpha_L^R d_R)\right] / \alpha_L^R. \tag{7}$$

β^T is the TPA coefficient of the two-photon absorber, β^R is the gain factor of the Raman-active material, R_R and R_T are the reflection coefficients of the Raman sample and the two-photon absorber at ω_L, respectively, and α_L^T and α_L^R are the corresponding linear-absorption coefficients at ω_L. K is a constant factor which depends on the linear optical parameters of the samples. For simplicity, we did not express the explicit dependence of I_p and I_L on x, y, and t. Here, the assumption has been made that the strong beam is attenuated only by one-photon absorption and has no significant back reflection.

The energy of the transmitted probe beam through the composite sample is given by the integral of $I_p(z = D)$ over the beam cross section and the pulse duration. From Eq. (7) it is seen that by measuring the NL transmission of the composite sample, information on β_{eff} may be obtained. No accurate *absolute* value for β_{eff} can be obtained because no detailed intensity profile of the laser beams and their spatial and time overlap are available. However, by scanning $\omega_L - \omega_p$ in the vicinity of a Raman-active mode of the Raman sample, the profile of the Raman gain may be used as an internal reference for calibrating β_{eff} and the TPA coefficient. In Fig. 3 we show the spectra of β_{eff} for liquid benzene and for a composite sample (benzene in series with CdS crystal) for $\omega_L - \omega_p$ in the vicinity of the 3063 cm^{-1} strong CH mode of benzene. In part (a) of Fig. 3, β_{eff} is positive, which means that there is a net gain in the vicinity of the Raman mode of the liquid. The interference between gain
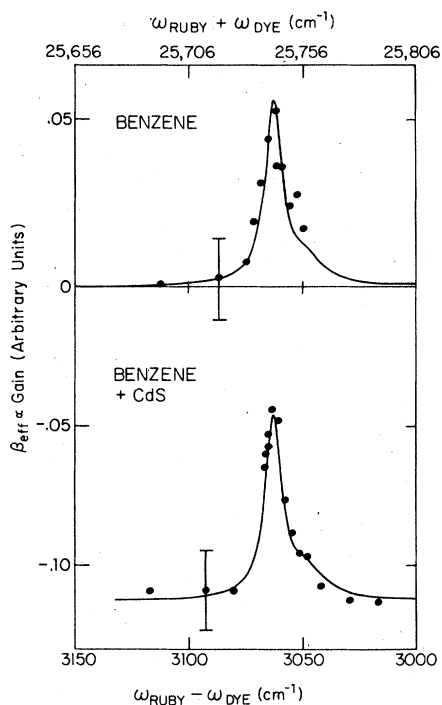
FIG. 3. Gain measurement vs the difference frequency in the vicinity of the 3063-cm^{-1} benzene Raman mode. The solid line is the spontaneous Raman spectrum of benzene obtained by using the 5145-Å line of argonion laser with spectrometer slit width of 0.4 cm^{-1}.

and loss in the composite sample is clearly shown in part (b) of Fig. 3. In addition to the experimental data of β_{eff} the spontaneous Raman line shape is also included in Fig. 3. The latter spectrum was normalized to fit the measured data of β_{eff}.

In an independent measurement, the linear dependence of the NL absorption (or gain) on the ruby intensity was verified for each sample. This measurement was performed by inserting calibrated filters in front of the sample. We have previously demonstrated[11] the usefulness of this procedure for obtaining relative TPA cross sections. The apparent NL gain or loss depends, of course, on the overlap of the probe and strong laser beam in the medium. To verify Eq. (7) and to check the reliability of the calibration measurement, we measured the Raman gain for different lengths of the active material. The expected linear dependence of the gain on the sample length has been found. An additional check was performed by measuring the TPA in thin samples placed at different distances from the Raman cell. No appreciable change in the effective TPA was found when the sample was translated by 5 cm. These experiments, the reproducibility of the Raman line shape for a benzene sample and for a benzene plus a two-photon

absorber composite sample, the good fit between the spontaneous Raman and the Raman-gain line shapes, all prove that the spectrum measured in the composite sample corresponds indeed to β_{eff}.

The peak intensity of the spontaneous Raman 3063-cm^{-1} mode of benzene was measured relative to that of the 2855-cm^{-1} mode of cyclohexane in a spontaneous Raman experiment. An absolute value for the cross section of the latter mode was given in Refs. 28 and 29.

The normalization measurement at twice the ruby frequency was performed using the same set-up as described above. Of course, no weak-probe beam is used in this experiment. A detailed discussion on the one-frequency normalization method is given in Refs. 11 and 12.

IV. RESULTS AND DISCUSSION

From the observed values of β_{eff}, the TPA coefficients β are derived from Eq. (7). These are plotted for GaP and CdS at 3.91, 3.56, and 3.18 eV in Fig. 1. Also shown in Fig. 1 is β for ZnSe at 3.18 and 3.56 eV. To obtain absolute TPA coefficients at 3.56 eV we used the measured ratio $\beta_{TiO_2}/\beta_{ZnSe} = 0.22$ at 3.56 eV and the TPA dispersion data given by Waff and Park.[30] From their data we obtained the ratio for the TPA coefficients in TiO$_2$ at 3.91 and 3.56 eV. Using this ratio and our absolute TPA measurement at 3.91 eV we obtained the absolute cross sections at 3.56 eV.

In addition, we found a very small TPA coefficient in SrTiO$_3$ at 3.56 eV ($\beta_{SrTiO_3} = 0.09\ \beta_{ZnSe}$). We also checked the glass filters Schott NG-10 and Corning 3-94 and 2-64 used as attenuators in the experiment. No TPA could be detected in these filters.

We will now compare our results with other reported TPA data and discuss the relation between the NL spectrum and the linear one. In CdS the TPA cross section decreases with increasing frequency (see Fig. 1). The magnitude of β is quite large. At 3.18 eV the value of β is about 0.1 cm/MW. Like the case of other materials in which the TPA properties were extensively explored, the reported TPA data on CdS show a variety of spectral characteristics. Several reports on the NL properties of CdS in the exciton region close to the band gap are available.[31] We will concern ourselves here, however, with the broad-band spectral measurements. In a recent publication by Penzkofer et al.[32] the TPA spectrum is smooth with a weak negative slope in the region 3–3.5 eV for laser electric field normal to the c axis. The reported value for the TPA cross section at 3.2 eV in this reference differs by about a factor of 4 from our measurement. An explanation for the

origin of the discrepancy between these two experimental methods is given in Ref. 11. Koren *et al.*[33] who have measured the two-photon induced fluorescence and Bespalov *et al.*[34] who have measured the attenuation induced by the TPA process have found, however, a positive dispersion in the region 3–3.5 eV. Koren *et al.*[33] report a singular structure in the spectrum of β in the vicinity of 3.2 eV. They attribute this feature to an allowed two-photon but forbidden one-photon transition. A measurement by Parson *et al.*[35] of $\chi^{(2)}$ also shows a rise in $\chi^{(2)}$ in the vicinity of 3.2 eV. Taking into account the selection rules of the second order susceptibility, this structure cannot be justified by the arguments used in Ref. 33 in explaining their TPA spectrum. Because our spectral region overlaps the other reported TPA measurements only partially, the present data do not resolve the discrepancies mentioned above. We note that the real part of the linear susceptibility is almost constant in the region 3–4 eV, while the imaginary part of $\chi^{(1)}$, which is quite small, increases moderately towards a strong peak at about 5 eV. Since no appreciable contribution to $\chi^{(1)}$ in this spectral region originates from critical points in the Brillouin zone we do not expect to find strong dispersion in $\chi^{(3)}$ unless some forbidden transitions play an important role in the NL case.[33]

In GaP the variation of β is very small (see Fig. 1). This fact is very interesting because very strong dispersion in $\chi^{(1)}$ was found in the region 3–4 eV.[21] A rise and a strong peak ("E_1 peak") in the spectrum of $\chi^{(1)}$ at about 3.7 eV is attributed to Λ^c–Λ^v transitions. According to band-structure theories, these transitions will contribute strongly to $\chi^{(1)}$ because the lowest conduction band and the upper valence band are very nearly parallel in the Λ direction for more than half the zone. This critical point along Λ may be approximated by a two-dimensional minima.[36] The contribution of the E_1 transition is also reflected by the strong rise in the region 3–3.6 eV found in a measurement of $\chi^{(2)}$ in GaP.[7] Since TPA transitions are allowed in the critical zone along Λ,[37] we expected to find strong dispersion in the TPA spectrum in the region of the measurement. In addition, since the TPA transition is also allowed in the critical point on the Σ axis, a critical point which is responsible for the broad and prominent peak at about 5 eV, we expected a larger value for β at 3.9 eV. A calculation of $\chi^{(3)}$ based on a detailed band structure may, however, fit the experimental data in spite of the qualitative arguments used here. Destructive interference between the contributions of different intermediate bands to $\chi^{(3)}$ or the contribution from impurity levels might explain the discrepancy between the linear and NL data.[26] The

NL data could be useful in improving band-structure models in the vicinity of the corresponding critical points. The absolute TPA cross section at 3.56 eV and comparative measurements in other crystals of the zinc-blende structure provides a check for such calculations. We have estimated the contribution from a second-order process to the effective TPA coefficient. By assuming that $\chi^{(2)}$ at 3.56 eV is complex[7] and consists of equal real and imaginary contributions, and by using the data for the dielectric constants from Ref. 38, we obtain for the second-order contribution the value $\beta \sim 1.2 \times 10^{-3}$ cm/MW. This expected contribution is quite small in comparison with the measured values of β, and therefore is not important.

A TPA measurement at 3.56 eV in GaP was also reported by Catalano *et al.*[39] Their result is about a factor of 3 smaller than the TPA cross section obtained here.

In ZnSe we measured β only at 3.56 and 3.18 eV. The data are shown in Fig. 1. The rise in β is consistent with the characteristics of $\chi^{(1)}$ that exhibit a small rise in the region 3.0–3.6 eV which is close to the crystal energy gap.[21] Other measurements of β in ZnSe at 3.56 eV are about a factor of 2 smaller than our measurements.[40] It is interesting to note that Arsenev *et al.*[41] found the ratio $\beta_{ZnSe}/\beta_{Cds} = 1.3$ which is very close to the ratio of 1.15 found in the present work.

As was mentioned previously, the Keldysh model predicts very small values for β, while Basov's model is close to the experimental results. The two models give different dispersion results for CdS. In Basov's model β rises to a peak at about 3.8 eV and then decreases moderately while Keldysh's model gives β with a monotonic rise up to 5 eV (see Fig. 1). In GaP and ZnSe, Basov's and Keldysh's models show similar dispersion behavior. In both crystals the TPA coefficients rise monotonically towards a plateau which begins at about 4 eV. The results of Basov's model are presented in Fig. 1. Keldysh's model gives dispersion which is very similar to that of CdS. It is not surprising that the Keldysh model, while yielding reasonable values for $\chi^{(1)}$, predicts too-small TPA coefficients. The important role of the intermediate states in the NL case is not adequately accounted for in the Keldysh model.

V. CONCLUSIONS AND SUMMARY

A new method for calibrating TPA versus Raman cross section is presented. Reliable TPA cross sections which are independent of the laser properties may be obtained. This method is especially useful for measuring broad TPA spectra utilizing different strong lasers. Because the Raman cross

section is the most reliable NL parameter available today, different third-order susceptibilities may be accurately calibrated versus Raman cross sections. We suggest that a comprehensive study of the absolute Raman cross sections of standard materials in a broad spectral region will be very useful.

Using the composite sample technique, we measured the TPA cross section of CdS, ZnSe, and GaP at 3.18 and 3.56 eV. The results of this measurement with our recent data at 3.91 eV show interesting characteristics concerning the band structure of the materials examined. The TPA data may be used to improve detailed band structure models. A calculation of the TPA coefficients using two simplified models were found, as expected, to be unsatisfactory. Calculations based on detailed models, e.g., the empirical pseudopotential model, should be done to get a better physical understanding of the TPA results.

By using a cw probe laser beam[42] a significant improvement of the TPA calibration techniques can be achieved. Very recently Owyoung[43] has shown that stimulated Raman spectra are obtainable using two cw lasers. An advantage of this cw technique over the pulsed techniques is that it is easier to obtain narrow-band cw lasers and thus narrow TPA features may be explored. In addition, strong and narrow Raman modes which are found over a wide range of the spectrum can be utilized for the TPA calibration. The use of stabilized cw probe laser beam and lock-in techniques may enhance the sensitivity by three orders of magnitude. Thus, interesting spectral features such as nonlinear absorption edges may be explored in spite of their weak cross section.

The TPA method discussed in this paper is based on NL attenuation of a probe beam in the sample. This kind of measurement is less reliable than the measurements based on coherent mixing processes[9,10] which are also connected with $\chi^{(3)}$. In the former measurement competing effects in the material may mask the TPA process, but they do not influence the coherent process. An accurate TPA measurement in solids based on coherent mixing processes is feasible[9] whenever the Raman cross section of the TPA material is available.

The spectral region of the measurement of $\chi^{(3)}$ based on TPA induced transitions is limited to the spectral region below twice the fundamental energy gap because of the one-photon absorption in the material. An extension of this spectral region may be achieved by measuring $|\chi^{(3)}|$ via four-wave mixing experiments of the type $\omega_{out} = 2\omega_1 + \omega_2$,[44] or by third-harmonic generation.[45] The real and imaginary parts may be measured in an interferometric method as had been demonstrated a decade ago for the case of $\chi^{(2)}$.[46]

---

*On leave from Universidade Federal de Pernambuco, Departmento de Fisica, 50000 Recife, Brazil.

†Present address: Tamam, Ben-Gurion Airport, Lod, Israel.

[1] D. Frohlich, Comments Solid State Phys. 4, 179 (1972); J. M. Worlock, in Laser Handbook, edited by F. T. Arecchi and E. O. Schulz-DuBois (North-Holland, Amsterdam, 1972), Vol. I, p. 1323; V. I. Bredikhin, M. D. Galanin, and V. N. Genkin, Usp. Fiz. Nauk. 110, 3 (1973) [Sov. Phys.-Usp. 16, 299 (1973)].

[2] H. Mahr, in Quantum Electronics, edited by H. Rabin and C. L. Tang (Academic, New York, 1975), Vol. I, p. 285; W. M. McClain, J. Chem. Phys. 55, 2789 (1971).

[3] N. Bloembergen, Nonlinear Optics (Benjamin, New York, 1965).

[4] P. D. Maker and R. W. Terhune, Phys. Rev. 137, A801 (1965).

[5] N. Bloembergen, Am. J. Phys. 35, 989 (1967).

[6] Chr. Flytzanis and N. Bloembergen, in Progress in Quantum Electronics, edited by J. H. Sanders and S. Stenholm (Pergamon, New York, 1976).

[7] H. Lotem and Y. Yacoby, Phys. Rev. B 10, 3402 (1974).

[8] A. Owyoung, Opt. Commun. 26, 266 (1976).

[9] M. D. Levenson and N. Bloembergen, J. Chem. Phys. 60, 1323 (1974); Phys. Rev. B 10, 4447 (1974).

[10] R. T. Lynch, Jr. and H. Lotem, J. Chem. Phys. 66, 1905 (1977).

[11] H. Lotem and Cid B. de Araujo, Phys. Rev. B 16, 1711 (1977).

[12] H. Lotem, J. H. Bechtel, and W. L. Smith, Appl. Phys. Lett. 28, 389 (1976).

[13] J. H. Bechtel and W. L. Smith, Phys. Rev. B 13, 3515 (1976).

[14] H. Lotem and R. T. Lynch, Jr., Phys. Rev. Lett. 37, 334 (1976).

[15] M. El-Sayed, F. M. Johnson, and J. A. Duardo, J. Chem. Phys. 64, 227 (1967).

[16]L. V. Keldysh, Zh. Eksp. Teor. Fiz. 47, 1945 (1964) [Sov. Phys.-JETP 20, 1307 (1965)].

[17]N. G. Basov, A. Z. Grasyuk, I. G. Zubarev, V. A. Katulin, and O. N. Krokhin, Zh. Eksp. Teor. Fiz. 50, 551 (1966)[Sov. Phys.-JETP 23, 366 (1966)].

[18]E. Yablonovitch, C. Flytzanis, and N. Bloembergen, Phys. Rev. Lett. 29, 865, (1972); J. P. Coffinet and F. DeMartini, ibid. 22, 60 (1969).

[19]S. D. Kramer and N. Bloembergen, Phys. Rev. B 15, 4654 (1976).

[20]T. K. Bergstresser and M. L. Cohen, Phys. Rev. 164, 1069 (1967); M. Cardona and G. Harbeke, ibid. 137, A1467 (1965).

[21]J. P. Walter and M. L. Cohen, Phys. Rev. 183, 763 (1969).

[22]S. S. Mitra, L. M. Narducci, R. A. Shatas, Y. F. Tsay, and A. Vaidyanathan, Appl. Opt. 14, 3038 (1975).

[23]P. Liu, W. L. Smith, J. H. Bechtel, H. Lotem, N. Bloembergen, and R. Adhav (unpublished).

[24]B. M. Ashkinadze, S. L. Pyshkin, S. M. Ryvkin, and I. D. Yanoshetskii, Fiz. Tekh. Poluprovodn. 1, 1017 (1967) [Sov. Phys.-Semicond. 1, 850 (1968)].

[25]C. Y. Fong and Y. R. Shen, Phys. Rev. B 12, 2325 (1975).

[26]G. Koren, Phys. Rev. B 11, 802 (1975).

[27]M. D. Levenson (private communication).

[28]M. J. Colles and J. E. Griffiths, J. Chem. Phys. 56, 3384 (1972).

[29]The Raman data on cyclohexane given in Ref. 28 had been used in Ref. 11. In a more recent paper [J. E. Griffiths, J. Chem. Phys. 60, 2556 (1974)] corrections for the Raman cross section in the region of 3000 cm^{-1} are discussed. Using the data given in the latter reference we corrected the Raman cross section of cyclohexane and accordingly the TPA data given in Ref. 11.

[30]H. S. Waff and K. Park, Phys. Lett. A 32, 109 (1970).

[31]R. G. Stafford and M. Sondergeld, Phys. Rev. B 10, 3471 (1974); R. W. Svorec and L. L. Chase, Solid

State Commun. 17, 803 (1975); V. T. Nguyen, T. C. Damen, and E. Gornic, Appl. Phys. Lett. 30, 33 (1977).

[32]A. Penzkofer, W. Falkenstein, and W. Kaiser, Appl. Phys. Lett. 28, 319 (1976).

[33]G. Koren, C. Cohen, and W. Low, Solid State Commun. 16, 257 (1975).

[34]M. S. Bespalov, L. A. Kulevskii, V. P. Makarov, M. A. Prokhorov, and A. A. Tikhonov, Zh. Eksp. Teor. Fiz. 55, 144 (1968) [Sov. Phys.-JETP 28, 77 (1969)].

[35]F. G. Parsons, E. Yi Chen, and R. K. Chang, Phys. Rev. Lett. 27, 1436 (1971).

[36]M. I. Bell, in Electronic Density of States, edited by L. H. Bennett (U.S. GPO, Washington, D. C., 1971), p. 757.

[37]M. Inoue and Y. Toyozawa, J. Phys. Soc. Jpn. 20, 363 (1965); T. R. Bader and A. Gold, Phys. Rev. 171, 997 (1968).

[38]B. O. Seraphin and H. E. Bennet, Semiconductors and Semimetals (Academic, New York, 1967), Vol. 3.

[39]I. M. Catalano, A. Cingolani, and A. Minafra, Solid State Commun. 16, 417 (1975).

[40]M. S. Brodin and D. B. Goer, Fiz. Tekh. Poluprovodn. 5, 256 (1971) [Sov. Phys.-Semicond. 6, 629 (1972)].

[41]V. V. Arsenev, V. S. Dneproskii, D. N. Klyshko, and A. N. Penin, Zh. Eksp. Teor. Fiz. 56, 760 (1969) [Sov. Phys.-JETP, 29, 413 (1969)].

[42]R. L. Swofford and W. M. McClain, Rev. Sci. Instrum. 46, 246 (1975).

[43]A. Owyoung, IEEE J. Quantum Electron. (to be published).

[44]J. A. Armstrong and J. J. Wynne, in Proceedings of the Enrico Fermi School, edited by N. Bloembergen (North-Holland, Amsterdam, 1977).

[45]W. K. Burns and N. Bloembergen, Phys. Rev. B 4, 3437 (1971).

[46]N. Bloembergen, R. K. Chang and J. Ducuing, in Physics of Quantum Electronics, edited by P. L. Kelley, B. Lax, and P. E. Tannenwald (McGraw-Hill, New York, 1966), p. 67.